Int. J. Multiphase Flow, Vol. 3, pp. 263–272. Pergamon/Elsevier, 1977. Printed in Great Britain.

AERODYNAMIC BEHAVIOR OF LIQUID SPRAYS

P. H. ROTHE and J. A. BLOCK

Creare Incorporated, Hanover, NH, U.S.A.

(*Received* 15 *November* 1975)

Abstract—An analysis is presented for the effect of entrained gas flows on drop trajectories and spray distributions from liquid atomizing nozzles. In particular, the effect of the pressure (or density) of the environment into which the liquid is sprayed is examined. The contraction of atomized sprays at elevated pressure which has been observed by various workers is explained, and the analysis is substantially confirmed by their data and by new data presented here. Both the data and the theory show that the amount of spray contraction increases with increasing ambient pressure and nozzle pressure drop, and decreases with increasing nozzle diameter and drop size. The theory examines the entrained gas flow around and into a spray and its subsequent effect on the trajectories of the liquid droplets comprising the spray.

INTRODUCTION

A liquid sprayed into a gas environment induces a gas flow which modifies the trajectories of the drops in the spray leading to contraction of the effective spray angle. DeCorso & Kemeny (1957), Neya & Sato (1968), and other investigators reported that such spray contraction increased as ambient pressure or nozzle pressure drop was increased. In this paper we examine the physical processes that lead to this contraction of liquid sprays.

The drop formation process with single-fluid, pressure atomizing nozzles has been widely studied, but much less attention has been given to the subsequent history of the resultant spray. The aerodynamic behavior of liquid sprays is of interest in numerous spray applications including spray dryers, super-charged boilers, gas-turbine combustors, and nuclear reactor spray systems for emergency core cooling.

When a liquid is sprayed into a non-condensing gas environment, momentum is exchanged between the liquid drops and the gas. Aerodynamic drag causes deceleration of the liquid drops, and the momentum lost by the liquid drops is acquired by the gas. Each of the drops in the spray acts roughly like a small drag pump. The power for these "pumps" is supplied by the original kinetic energy of the spray and by gravity. The pumping energy pulls the gas along, thus creating a flow field where gas is continually entrained into the spray. As the entrained gas enters the spray, it drags the liquid drops at the outer regions of the spray inward, causing the spray to contract. The magnitude of the contraction depends on how effectively the spray drops entrain gas, and on how strongly the inflowing gas pushes the drops from their original trajectories. These effects in turn depend on such parameters as original spray kinetic energy (set in part by nozzle pressure), total flow rate, drop size, and gas density (which depends on environmental pressure).

ANALYSIS

The effects of gas entrainment on spray behavior are analyzed in two steps. First, the liquid velocity and the velocity of the gas entering the spray cone are determined as functions of axial position. These results are then used to calculate the trajectory of a drop on the spray envelope, and hence the contraction of the spray as a function of axial distance from the nozzle.

Experiments by the authors reported later in this paper and those of Binark & Ranz (1958) have shown that the gas enters the spray roughly perpendicular to the trajectory of the outer spray droplets. Because the trajectories are unknown initially, the entrained gas velocities are calculated with the approximation that the gas enters perpendicular to the cone defined by the initial spray angle at the nozzle. The drop trajectories are subsequently calculated without this approximation. In principle, the entrained gas velocities and drop trajectories could be recalculated iteratively. This degree of computational complexity is warranted only for large spray contraction angles and has not been introduced in the present analysis.

Gas entrainment

Gas and liquid flows inside the spray are treated as steady, uniform and one-dimensional. The film region of the spray, very near the orifice, is not considered in this analysis. Gravity and all other body forces are neglected, and chemical reactions, condensation or evaporation are not considered. Figure 1 illustrates the geometry and nomenclature of this analysis.

The velocity of the gas entering the spray $V_{Gc}(x)$ may be related to the gas velocity inside the spray $V_G(x)$ by continuity for the gas phase, neglecting the volume occupied by the liquid drops,

$$\int_0^x \frac{2\pi R V_{Gc}}{\cos\theta_c}\,dx = \pi R^2 V_G. \qquad [1]$$

An approximate axial-momentum balance may be written for both phases (simultaneously) using the control volume sketched in figure 1. For convenience, it may be assumed that the drop velocities are purely axial. A more rigorous treatment that considers the actual trajectory angles of the drops reduces to [2] obtained below. All surfaces of the control volume are far from the nozzle except for the surfaces which intersect the spray. Assuming that the pressure is everywhere equal to the ambient pressure on the control surface, the axial-momentum balance is expressed by

$$W_L V_{L0} = W_L V_L + \pi R^2 \rho_G V_G^2 \qquad [2]$$

where W_L is the mass flow rate of liquid and ρ_G is the gas density.

Normalized gas and liquid velocities are defined by $V_G^* = V_G/V_{L0}$ and $V_L^* = V_L/V_{L0}$. A normalized axial position is $x^* = x/x_0$, where the length scale, $x_0 = [(4/\pi)(W_L/\rho_L V_{L0})]^{1/2}$, is equal to the orifice diameter of a nozzle having unity contraction coefficient. Differentiating[1] with respect to x and noting that $R = x\tan\theta_c$, the continuity and axial momentum equations may be written in normalized form

$$V_{Gc}^* = \frac{\sin\theta_c}{2x^*}\frac{d}{dx^*}[x^{*2}V_G^*], \qquad [3]$$

$$mx^{*2}V_G^{*2} + V_L^* = 1. \qquad [4]$$

The parameter $m = 4(\rho_G/\rho_L)\tan^2\theta_c$ is a known product of the density ratio and a spray geometry term.

The third relation needed to determine the three normalized velocities V_G^*, V_L^*, and V_{Gc}^* may be obtained from an equation expressing the interaction between the liquid drops and the gas inside the spray envelope. We consider two cases.

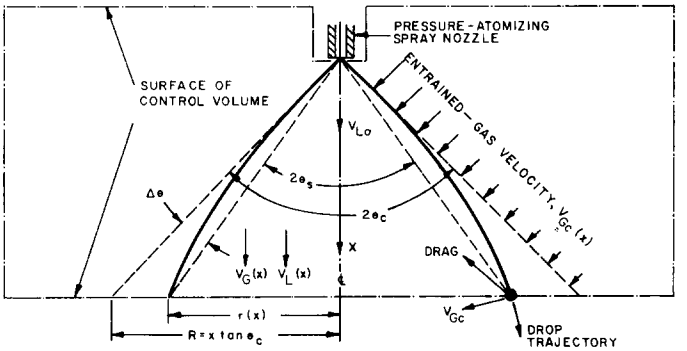

Figure 1. Control volume for analysis.

First, if the limiting case of no relative velocity between the phases inside the spray is assumed, then $V_G^* = V_L^*$, and the axial-momentum equation can be solved in closed form to obtain

$$V_G^* = V_L^* = \frac{(1+4mx^{*2})^{1/2}-1}{2mx^{*2}}. \quad [5]$$

Inserting this relation into the continuity equation gives

$$V_{Gc}^* = \frac{\sin\theta_c}{(1+4mx^{*2})^{1/2}}. \quad [6]$$

More generally, the relative velocity between the phases may be expressed by the drag equation

$$(\pi/6)D^3\rho_L(\mathrm{d}V_L/\mathrm{d}t) = -C_D(\pi/4)D^2(\rho_G/2)(V_L - V_G)^2 \quad [7]$$

where D is a representative drop size and C_D is an appropriate drag coefficient. Using $\mathrm{d}V_L/\mathrm{d}t = V_L(\mathrm{d}V_L/\mathrm{d}x)$ and normalizing the drag equation gives

$$V_L^*(\mathrm{d}V_L^*/\mathrm{d}x^*) = -(V_L^* - V_G^*)^2/\delta^* \quad [8]$$

where $\delta^* = \delta/x_0 = (4/3C_D)(\rho_L/\rho_G)(D/x_0)$ is a normalized relaxation length for the drops.

The drag equation [8] and the axial-momentum equation [4] were simultaneously solved numerically to obtain plots like those of figure 2. The solution with no relative velocity, [5], is also shown. The corresponding inflow velocities (obtained using [3]) are shown in figure 3. (Some of the lines in figures 2 and 3 with relative velocity actually do cross the line of no relative velocity slightly as shown.) These solutions were obtained with constant relaxation length. Later calculations of spray contraction treat relaxation length as a dependent variable.

Drop trajectories

Only the ratio of the liquid velocity to the inflow velocity V_L/V_{Gc} is necessary to determine the trajectory of a drop on the spray envelope. The instantaneous radius of curvature ζ of a drop trajectory may be related to the component of the drop acceleration normal to its trajectory, a_n, by $1/\zeta = a_n/V_L^2$, where V_L is the velocity of the drop. In terms of the radial position r of the

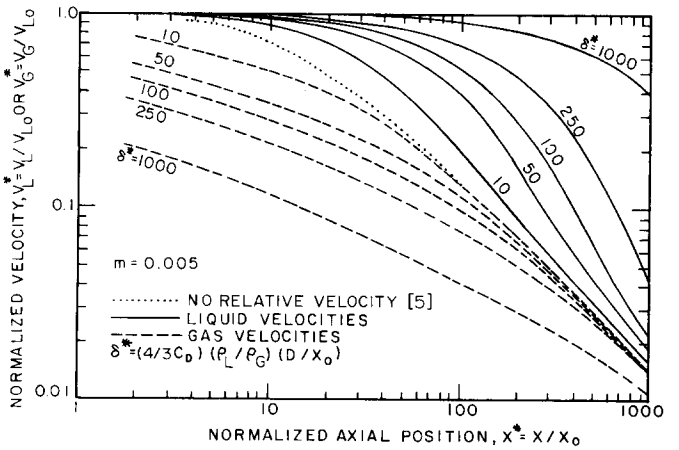

Figure 2. Calculated liquid and gas velocities in a spray.

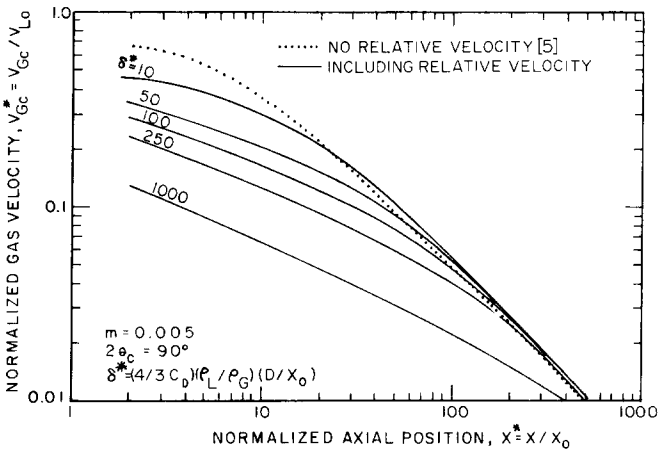

Figure 3. Calculated gas velocities entering the spray.

spray envelope, this trajectory equation becomes

$$[1+(dr/dx)^2]^{-3/2}\, d^2r/dx^2 = -a_n/V_L^2 \qquad [9]$$

The spray angle θ_s may be determined from $\tan\theta_s = r/x$ and the spray contraction angle is $2\Delta\theta = 2\theta_c - 2\theta_s$.

The component of acceleration normal to the drop trajectory is obtained by a force balance on the drop which gives

$$a_n = \frac{C_D[(\pi/4)D^2][(\rho_G/2)(V_L^2+V_{Gc}^2)]}{(\pi/6)D^3\rho_L}\,\frac{V_{Gc}}{\sqrt{(V_L^2+V_{Gc}^2)}} \qquad [10]$$

where $\sqrt{(V_L^2+V_{Gc}^2)}$ is the relative velocity between the drop and the incoming gas phase.

Inserting this expression for acceleration [10] into the drop trajectory [9] gives

$$[1+(dr/dx)^2]^{-3/2}\, d^2r/dx^2 = (V_{Gc}/\delta V_L)\sqrt{(1+(V_{Gc}/V_L^2))} \qquad [11]$$

Later in this paper, [11] is used to determine the drop trajectory, and thereby to calculate the amount of spray contraction. The velocity ratio V_{Gc}/V_L is obtained from [3], [4], and [8] for the general case with relative velocity in the spray.

COMPARISON WITH EXPERIMENTS

Gas flows

Air-velocity data representative of several experiments described below are compared in figure 4 to the gas-entrainment analysis. A normalized relaxation length of $\delta^* = 100$ was used for this comparison and is an adequate approximation to all tests shown. Acceptable agreement is obtained for velocity magnitudes and overall trends though there is considerable scatter in the data due to the difficulty in measuring the inflow velocity.

Binark & Ranz (1958) tested one solid-cone and six hollow-cone water sprays in air at atmospheric pressure. They visualized the air flows using smoke and also obtained air-velocity countours using a pitot probe inside the spray and a hot-wire probe outside the spray. Briffa & Dombrowski (1966) studied a flat spray of iso-octane in air at atmospheric pressure. They took double-flash photographs of 30 μ lycopodium dust particles suspended in the air stream to determine the air velocity distributions inside and outside their sprays. Gluckert (1962) and Nakakuki (1973) also provide air velocity measurements inside sprays.

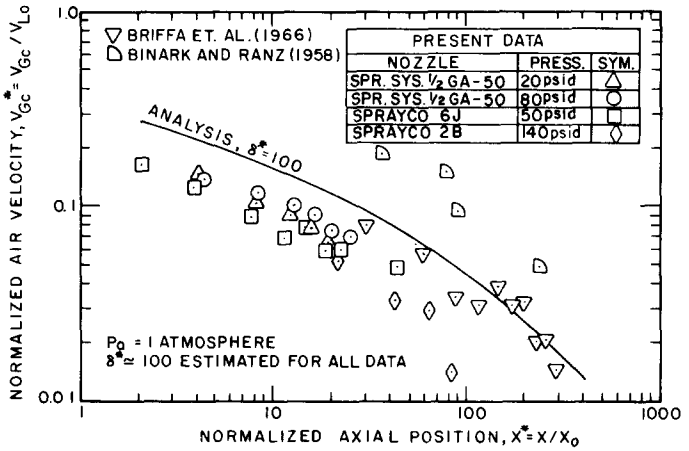

Figure 4. Axial variation of air inflow velocity.

Several solid-cone sprays of water in air were studied by the authors in order to assess various measurement techniques and to provide entrainment data using nozzles of somewhat larger size than previously studied. The air flows were visualized using smoke and falling thistle-down tufts. The air velocity on the spray envelope was determined using double-flash photographs of the tufts, a pitot probe, and by measuring the static pressure on a sharp-edged flat plate held parallel to the gas inflow velocity. All of these methods were employed outside the spray, nominally at the spray surface.

The static pressure inside the spray was measured under a small umbrella and the measurements were corrected for the umbrella wake by calibration in an air jet. We found that the static pressure inside the spray was below ambient pressure, in agreement with the data of DeCorso & Kemeny (1957) and others.

Our flow-visualization studies and the data of Binark & Ranz demonstrate that air enters the spray envelope nearly perpendicular to the drop trajectories and then turns rapidly to the axial direction as it passes into the spray. The hypothesis by DeCorso & Kemeny (1957) of a recirculating gas flow pattern (inside a hollow-cone spray) is probably incorrect.

We also tested various methods to measure velocities inside sprays, including photographic techniques and a pitot probe (having large taps to prevent obstruction and with tanks to collect the impinging water and keep the connecting lines free of water). We concluded that reliable measurements can be made outside sprays, but that velocity measurements inside sprays are often grossly inaccurate.

Spray distribution data

DeCorso & Kemeny (1957) and Neya & Sato (1968) each conducted similar spray-distribution measurements at elevated ambient pressures. The experimental conditions of these studies are shown in Table 1. DeCorso & Kemeny measured their spray distributions using an array of

Table 1. Experimental conditions of spray distribution studies

	DeCorso & Kemeny (1957)	Neya & Sato (1968)
Nozzle pressure drop Δp_N (psid)	25–400	75–600
Ambient pressure p_a (psia)	1.5–115	4–75
Orifice diameter d_0 (inch)	0.032–0.12	0.047
Initial spray angle $2\theta_c$ (deg.)	45–80°	70°, 90°, 110°
Measuring station x_m (inch)	4.5	7.9
Normalized position x_m/d_0	40–150	160
Liquid	iso-octane	water
Gas	Nitrogen	air

collection tubes. Neya & Sato collected sets of droplet samples using an immersion method in oil to catch the drops. These samples permitted Neya & Sato to determine both the spray distribution and the drop sizes.

Each investigator reduced his raw spray-distribution data to equivalent spray angles. Typical data are presented in this form in figures 5 and 6. The $p_a = 0$ line results from extrapolation of the spray angle data to zero ambient pressure (as illustrated in figure 6).

As described below, we followed the procedure established by Neya & Sato (1968) to reduce equivalent spray angles to spray contraction angles suitable for comparison to the present analysis. At high nozzle pressure only drag-induced spray contraction is important, but at low nozzle pressure gravity effects and decreased initial spray cone angle augment drag-induced spray contraction. We eliminated these low-nozzle-pressure effects, in order to isolate drag-induced spray contraction, by subtracting the equivalent spray angles from the $p_a = 0$ line (see figure 5). The resultant contraction angles are compared with the analytical predictions.

After all the data were reduced, one nozzle representative of those tested by each investigator was chosen and the corresponding data were compared with the theory. The DeCorso & Kemeny

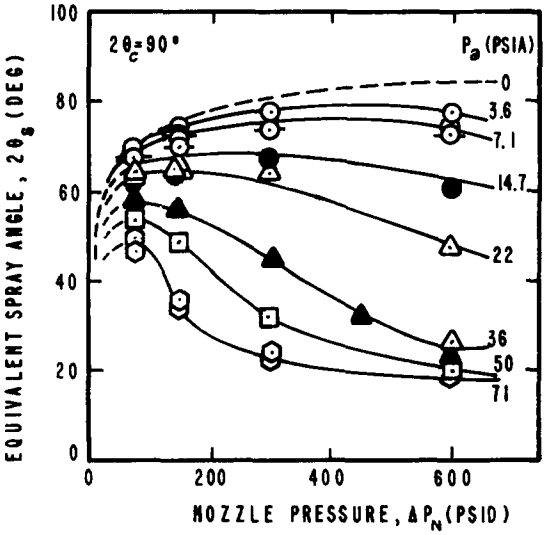

Figure 5. Equivalent spray angle data of Neya & Sato (1968).

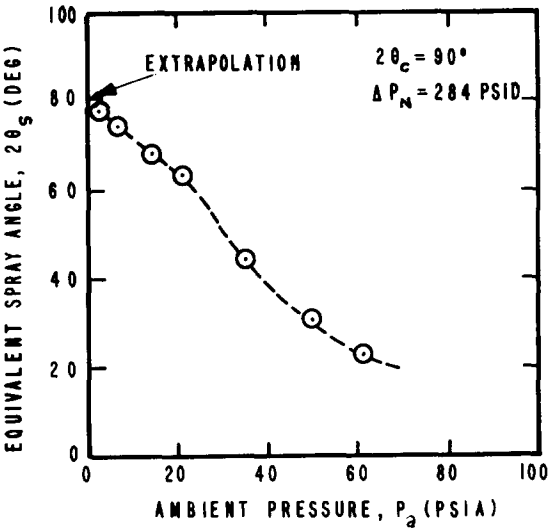

Figure 6. Data of Neya & Sato (1968) illustrating their procedure for extrapolating to zero ambient pressure.

nozzle had $2\theta_c = 45°$ and a mid-range orifice diameter $d_0 = 0.083$ inch; the Neya & Sato nozzle had a mid-range initial spray angle $2\theta_c = 90°$.

Comparison with spray distribution data

Guided by the analysis, we plotted the spray-contraction-angle data and the theory as a function of pressure product $(\Delta p)_N^{1/2} p_a$ (figure 7). Because the constant powers chosen in this pressure product are not exactly those resulting from the analysis, a family of curves was obtained as a function of nozzle pressure. Only a representative line is plotted in figure 7 because the variation in $\Delta\theta/\theta_c$ among the family of curves (at fixed $(\Delta p)_N^{1/2} p_a$) is less than the scatter in the data.

Acceptable agreement is achieved between the analysis and the data for spray contraction ratios in the range $\Delta\theta/\theta_c = 0.1$ to 0.6. At lower spray contraction ratios the experimental data are highly uncertain and at high spray contraction ratios the analysis breaks down because the gas inflow velocity is calculated assuming a conical spray (i.e. neglecting the contraction).

Some further limited calculations were performed to give rough comparisons of the theory with the data from the other nine nozzles of DeCorso & Kemeny. The theory and data appear to agree that the spray contraction ratio is relatively insensitive to the initial spray angle in the range tested. There is disagreement concerning the effect of orifice diameter. The calculations suggest that spray contraction ratio decreases inversely as a function of orifice diameter; the data of DeCorso & Kemeny appear to be insensitive to orifice diameter. However, some unpublished data obtained with large nozzles suggest that the calculated dependence on orifice diameter is correct in some cases. The theory also shows that spray contraction angles are inversely proportional to roughly the square of the drop size in a mono-dispersed spray.

Parameters used for comparisons with data

In order to obtain the theoretical curves of figure 7 it was necessary to postulate several interrelationships among the parameters. The six parameters needed to execute the gas-entrainment analysis are: ρ_G, ρ_L, $2\theta_c$, C_D, D and x_0. The readily available information from the

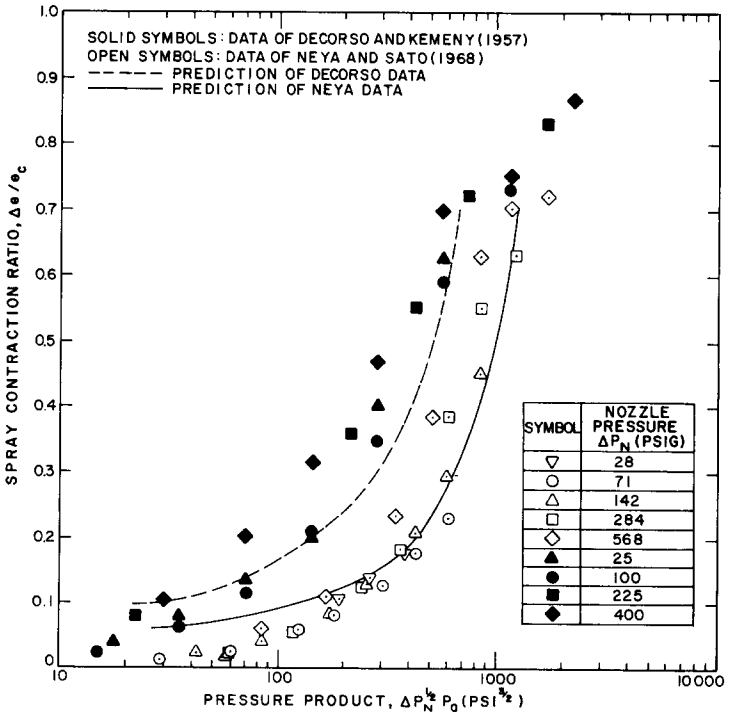

Figure 7. Comparison of spray contraction analysis and data.

experiments of DeCorso & Kemeny (1957) and Neya & Sato (1968) include ρ_L, $2\theta_c$, p_a, Δp_N, and d_0. Gas density was determined from measured ambient pressure using the perfect gas law and assuming 70°F room temperature. The remaining parameters were obtained as described below.

For C_D, we used the correlation presented by Schlicting (1968) of drag coefficient as a function of Reynolds number for flow over solid spheres. For numerical convenience, this correlation was approximated by three power-law segments. The data of Ingebo (1954) suggest only a minor refinement to this correlation, which we did not implement, in order to treat unsteady flow of clouds of liquid drops. We used a Reynolds number $Re_D = \rho_G DV/\mu_G$ where V was either $(V_L - V_G)$ or $\sqrt{(V_L^2 + V_{Gc}^2)}$ as appropriate. V varies as a function of axial position. To convert normalized velocities V^* (obtained from the gas-entrainment analysis) to dimensional velocities $V = V^* V_{L0}$, the initial liquid velocity was estimated from the nozzle pressure assuming unity velocity coefficient of the nozzle, $V_{L0} = \sqrt{(2(\Delta p)_N/\rho_L)}$.

To determine D, the drop-size correlation of Dombrowski & Wolfsohn (1972) was modified to the form,

$$D(\text{in}) = 0.126 \frac{[d_0(\text{in})]^{2/3}}{[\Delta p_N(\text{psid})]^{1/3}} \qquad [12]$$

This expression agreed well with the limited data of DeCorso (1960) and we applied it directly to his cases. The drop sizes measured by Neya & Sato (1968) were roughly a factor of 1.4 larger than predicted by this correlation. We used the measured drop size data of Neya & Sato in the comparison with their spray distribution data.

For circular orifices, the length scale is related to the orifice diameter by $x_0 = C_c^{1/2} d_0$ where C_c is the contraction coefficient of the nozzle. The present comparisons assume contraction coefficients of unity.

It was also assumed that ambient pressure had no effect on either drop size or *initial* spray cone angle. The photographs of Neya & Sato (1968) and DeCorso (1960) demonstrate that the initial spray cone angle is unaffected by ambient pressure. The effect of ambient pressure on drop size is less clear, but this effect appears to be weak and unimportant. Muraszew (1947), Bower (1948), Giffen & Lamb (1953) and Nakakuki (1973) report drop size as a function of ambient pressure. However in the range from 10 to 500 psia, most investigators reported less than a 40% range of drop size. Various sets of data have various conflicting trends, and one is led to believe that ambient pressure has a weak effect on drop size. Moreover, the data of Neya & Sato demonstrate that increased drop size at high ambient pressure results from coalescence of fine drops driven to the axis of strongly contracted sprays. This effect is of secondary importance to modeling spray contraction. Thus, in order to apply the present analysis, it is reasonable to assume that both drop size and initial spray cone angle are independent of ambient pressure.

DISCUSSION

The agreement between the analysis and the data shown in figures 4 and 7 is much better than might be expected considering the several analytical and modeling assumptions which were made. Most of the important features of the aerodynamic analysis have been confirmed by the available data. We claim that the theory presented here provides a useful tool for estimating both the contraction of a spray and the aerodynamic flow field induced by a liquid spray.

The amount of spray-contraction increases roughly linearly as a function of ambient pressure and increases somewhat more gradually as a function of nozzle pressure. Predicted spray-contraction angles agree well with the two sets of data reported in the literature. The factor of three difference between these sets of data as shown in figure 7 is due principally to the different drop-size distributions of the nozzles studied by the two investigators.

The measured velocities of the entrained gas entering the spray cone decay with axial position, as predicted by the analysis. Agreement between the analysis and this data is

acceptable. More comprehensive velocity data, particularly including cases in air at elevated ambient pressure, would provide a useful further test of the analysis.

Several uncertainties exist in the present analysis. The actual gas flow is strongly two-dimensional and non-uniform, as demonstrated by the data of Binark & Ranz (1958), Rabash & Stark (1962), and Briffa & Dombrowski (1966). Momentum considerations alone suggest that the actual average entrained-gas velocity is perhaps a factor of two lower than predicted by the present one dimensional gas entrainment analysis. Moreover, drops at the periphery of the spray travel through a nominally stagnant gas, and hence should slow disproportionately, while drops on the spray axis travel in a region of high relative gas velocity. Similarly, the present analysis neglects pressure terms in the momentum balance; a more complete treatment might increase predicted gas velocities by a factor of two. A two-dimensional analysis is needed to eliminate these uncertainties, but we do not expect a significant improvement in the accuracy or reliability of the predictions if the model is refined in this manner. The net uncertainty due to the above assumptions is probably within a factor of two if drop size is known accurately, whereas drop size is often uncertain by a factor of two and thus leads to roughly a factor of four error in predicted spray contraction.

The analysis could also be refined by iterating the gas-entrainment and drop trajectory steps of the analysis, by treating the actual drop size distributions, or by modeling the film region of the spray. At present these possible refinements appear less promising than improving correlations of drop size or extending the model to treat sprays in a condensable gas.

The data comparison reported here fails to provide a test for the effect of gravity on a vertical spray. We included the effect of gravity in another aerodynamic analysis and correctly predicted a negligible effect on the vertical sprays tested by Neya & Sato (1968). It may be more useful to several applications to extend the aerodynamic analysis, and to obtain test data, in order to model the combined effect of gravity and drag on nominally horizontal sprays.

CONCLUSIONS

A first-order understanding has been achieved concerning key fluid-dynamic processes governing contraction of liquid sprays. The analytical model unifies existing data and provides a competent predictive method for spray contraction and for the flow fields induced by a liquid spray in a gas environment.

Acknowledgements—We thank Professor Graham B. Wallis for reviewing this analytical model and focusing our attention on its strengths and weaknesses. The authors also wish to acknowledge the support of the Nuclear Energy Division of the General Electric Company in this study.

REFERENCES

BINARK, H. & RANZ, W. E. 1958 Induced air flows in fuel sprays. ASME Paper 58-A-284.

BOWER, H. 1948 The effects of cone angle, pressure and flow number on the particle size of a pressure jet atomizer. Shell Development Co., Tech. Rep. ICT/17.

BRIFFA, E. J. & DOMBROWSKI, N. 1966 Entrainment of air into a liquid spray. *A.I.Ch.E.Jl.* **12**, 708–17.

DECORSO, S. M. 1960 Effect of ambient and fuel pressure on spray drop size. *J. Engng Pwr* 10–18.

DECORSO, S. M. & KEMENY, G. A. 1957 Effect of ambient and fuel pressure on nozzle spray angle. *J. Engng Pwr* 607–17.

DOMBROWSKI, N. & WOLFSOHN, D. L. 1972 The atomization of water by swirl spray pressure nozzles. *Trans. Instn Chem. Engrs* **50**, 259–69.

GIFFEN, E. & LAMB, T. A. J. 1953 The effect of air density on spray atomization. The Motor Industry Research Association, Rep. 1953/5 (Great Britain).

GLUCKERT, F. A. 1962 A theoretical correlation of spray-dryer performance. *A.I.Ch.E.Jl.* **8**, 460–466.

INGEBO, R. D. 1954 Vaporization rates and drag coefficients for iso-octane sprays in turbulent air streams. NACA TN-3265.

MURASZEW, A. 1947 Fuel injection in internal combustion engines and fuel spray phenomena. The Motor Industry Research Association (MIRA) Rep. 1947/R6.

NAKAKUKI, A. 1973 Properties of sprays injected into compressed atmospheres. ASME Paper 73-WA/FE-18.

NEYA, K. & SATO, S. 1968 Effect of ambient air pressure on the spray characteristics of swirl atomizers. Ship Research Inst., Tokyo, Japan.

RABASH, D. J. & STARK, G. W. V. 1962 Some aerodynamic properties of sprays. *Chemical Eng., Lond.* A83–88.

SCHLICHTING, H. 1968 *Boundary Layer Theory*, 6th Ed. McGraw–Hill, New York.